

Computational Fluid Dynamics for the Design of New Generation Aircraft

1 Introduction

The project will first begin with the modeling, computation and design of the new generation of airliners, acronymed BWB (blended wing body). The methodology and the CFD technology can be further extended and generalized to other major new high performance and/or *hypersonic* aircraft designs.

This research project will provide the state-of-the-art computational fluid dynamics (CFD) training to the PhD students and postdocs at Texas A&M University. The research outcomes have the potential to be published at elite journals such as *Nature* and *Science*, and other high-impact factor journals.

2 BWB Airliners

The BWB, also called *hybrid wing*, *flying wing*, is characterized by a lift generation center-body and is an innovative aircraft configuration, compared with conventional tube and wing for transport aircraft. Because of the large area of wings, it promises a high lift/drag (L/D) ratio that can dramatically enhance the fuel-savings and performance.

Images of concept BWB aircraft are shown in Figures 1 and 2.

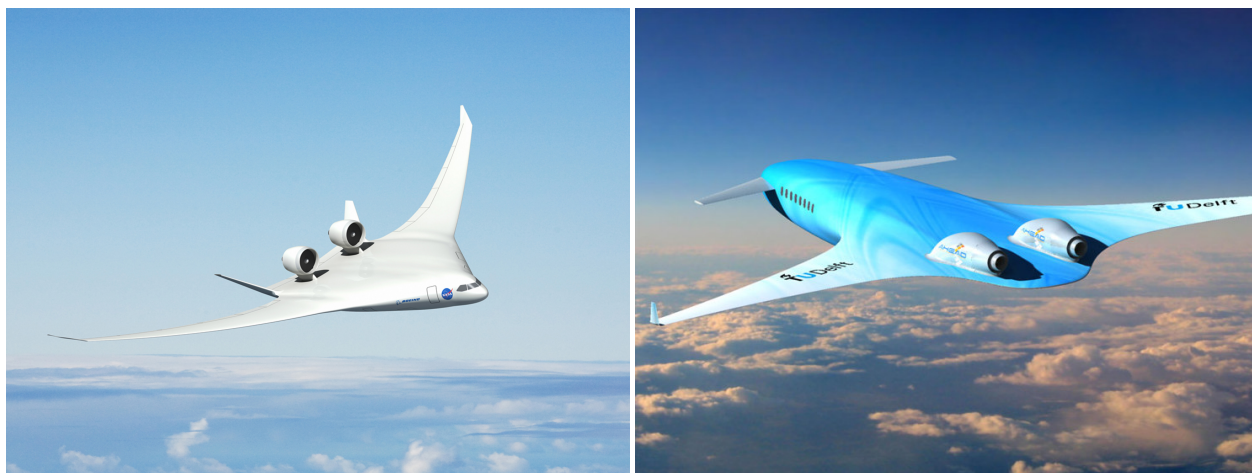


Figure 1: Left figure shows a rendered blended wing body concept by NASA and Boeing (Credit: NASA/Boeing). Right figure shows rendered concept designed by KLM and TU Delft (Credit: KLM/TU Delft).

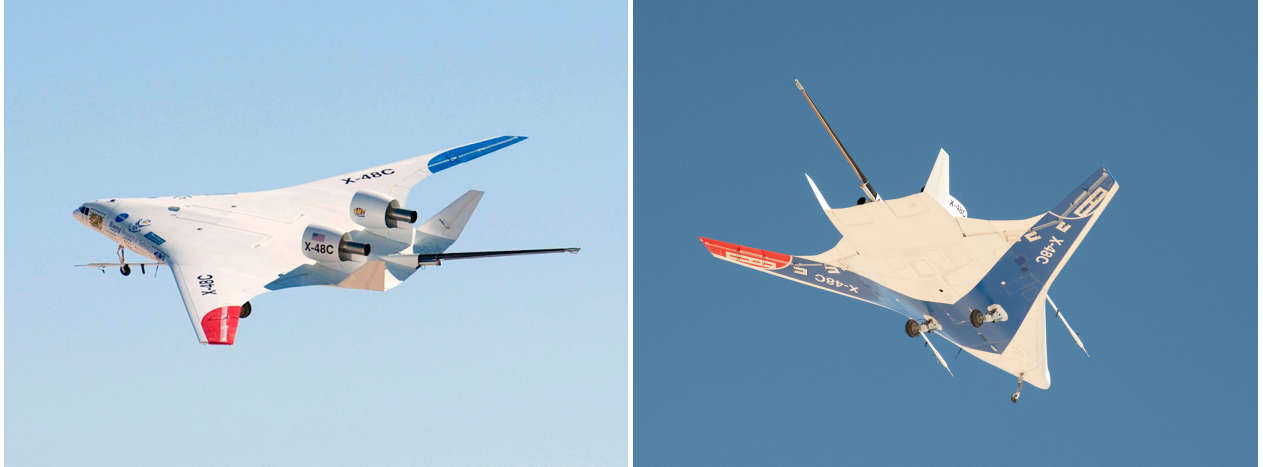


Figure 2: X-48C, a sub-scale technology demonstrator developed by Boeing and NASA, during a test flight on Feb. 28, 2013 [1] (Credit: NASA/Carla Thomas)

2.1 Overview of BWB Projects and Aerodynamics Research

During the late 1990s and early 2000s, Boeing, NASA and several U.S. universities, including Stanford and South California, conducted a series of research regarding blended wing body design, as discussed, for example in [2]. The Multidisciplinary Design Optimization (MDO) code, called WingMOD, was described in [3]. The aerodynamic aspect was discussed in [4], where CFD results were compared with wind tunnel data. A 6% scaled BWB aircraft was built at Stanford and two 8.5% scaled technology demonstrators known as Boeing/NASA X-48B and X-48C were built and put into test flights from 2007 to 2013 [1]. Figure 2 shows photos captured during a test flight of X-48C.

A project known as Multidisciplinary Optimization of BWB (MOB) was conducted during the early 2000s as a European Commission funded collaborative effort between several European universities and agencies, including Cranfield University in the U.K. and Technical University Delft (TU Delft) in the Netherlands, as summarized in [5]. Aerodynamic considerations, CFD, and shape optimizations are discussed, for example, in [6, 7]. Starting from around 2005, the silent aircraft initiative (*SAI*) by MIT and The University of Cambridge studied BWB configurations with a focus on noise reduction [8]. The path was later adopted by NASA to study propulsion system configurations and noise shielding, for example, in [9]. CFD simulation involving the engine was conducted in [10].

A French project AVECA, a collaboration between Airbus France and ONERA (Office National d'Etudes et de Recherches Aérospatiales), studied BWB configurations and aerodynamics, including CFD simulation, for example, in [11]. Adjoint based aerodynamic shape optimization was specifically addressed in [12].

Apart from the projects mentioned above, TsAGI in Russia designed a BWB aircraft in a project funded by Airbus and Boeing in [13]. Recently, several BWB configurations were conceptually designed by TU Delft in [14]. CFD driven aerodynamic shape optimization was explored in [15] in Israel, followed by [16] from the University of Toronto, [17] from Beihang University in China, and [18] from the University of Michigan, etc. The history and perspective of the BWB idea are also summarized in [19].

We have already carried out some preliminary computation of N2A-EXTE airframe using a mesh generated by STAR-CCM+ and solver `rhoSimpleFoam`, see Figure 3.

3 CFD Methodology and Applications to New Aircraft Design

Here, we give a brief description to our CFD approach. It is mainly based on the open-source software *OpenFOAM*, but with significant extra algorithmic and programming work done by us, with some combined

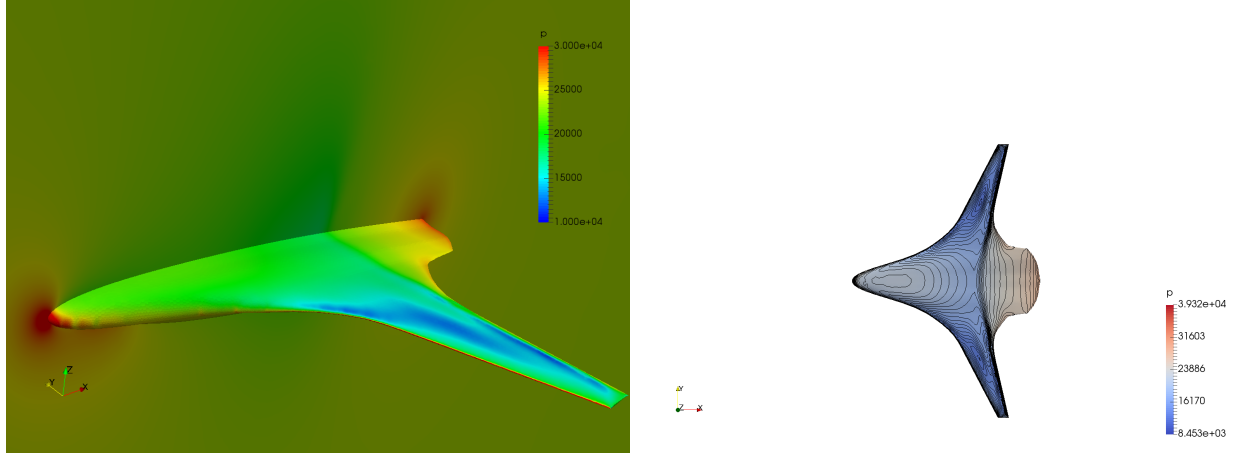


Figure 3: The pressure distribution of Blended Wing Body aircraft N2A-EXTE. The left figure shows pressure on aircraft body and along the central cross section. The right figure shows the pressure contour on the upper surface.

use of commercial software.

3.1 OpenFOAM Solvers and Validation: Compressible Solvers in OpenFOAM

OpenFOAM is a widely used open source-library for computational fluid dynamics [20, 21]. The focus of Navier-Stokes solvers in the OpenFOAM are largely pressure-based methods, while density-based solvers, which are considered more suitable for solving high-speed compressible flow is relatively less explored. Compressible solvers in standard OpenFOAM are summarized in Table 1. The solver `rhoCentralFoam` is the only density-based solver in Table 1, which uses central-upwind schemes of Kurganov and Tadmor [22]. There are several compressible solvers distributed in foam-extend or separately, including `dbnsFoam` which is a density-based Runge-Kutta transient solver, and `densityBasedTurbo`, which uses Godunov type schemes.

Solver	Time	Note
<code>rhoSimpleFoam</code>	steady	pressure-based
<code>rhoPimpleFoam</code>	transient	pressure-based
<code>sonicFoam</code>	transient	pressure-based
<code>rhoCentralFoam</code>	transient	density-based

Table 1: Summary of compressible solvers in standard OpenFOAM

At this stage, only standard OpenFOAM solvers are tested for either steady or pseudo-transient simulation.

3.2 Mesh Generation

Mesh quality greatly affect stability and accuracy of CFD simulations, and is important for intricate geometries in aerodynamic applications. Usually, near-wall regions need thin mesh layers to resolve the viscous boundary layer. The standard mesh generation tools in OpenFOAM have difficulty in reliably generating mesh near the wall to arbitrary thickness.

Additional meshing tools are developed to reliably generate hexahedral mesh with good mesh orthogonality and thickness control in the OpenFOAM platform. First, a multi-block transfinite surface mesh is

generated for the wing geometry. See Figure 4. Then, the O-topology mesh is extruded from the surface using ideas from hyperbolic mesh generation [23]. See Figure 5, with more details in Figure 6.

3.3 Validation against ONERA M6

The ONERA M6 wing panel was built and tested in a wind tunnel in 1979 [24]. Details of the geometry and test conditions can be found along the original test data. In particular, the wing operates under a transonic flow condition with Mach number $M = 0.8395$, which is close to typical modern passenger aircraft. The ONERA M6 wing has been and continues to be a standard validation case for CFD codes. In particular, both steady and local time-stepping pressure-based solvers in OpenFOAM have been tested [25,26]. In the current test, using the mesh described in Subsection 3.2, the pressure-based solver `rhoSimpleFoam` with upwind convection scheme is run until convergence. The $k-\omega$ SST turbulence modeling is used. See Figure 7 in the Appendix.

At this point, we have not yet succeeded in getting any *higher order convection schemes* to produce converged result, as they are less stable and less tolerant to mesh quality problems, especially for a steady solver. We started with the converged result as initial condition, `rhoCentralFoam` is then used to achieve second order accuracy. As a transient solver, `rhoCentralFoam` is subject to the constraint of the CFL condition, which makes the simulation very time consuming. The pressure coefficient contour of the converged result of `rhoSimpleFoam` and the final result of `rhoCentralFoam` are displayed in Figure 7, and pressure coefficient curves along various span locations are plotted in comparison with the experimental data in Figure 8 in the Appendix. It can be observed that the first order steady state solution fails to capture any shock, but it still serves as a good initial condition for further simulations. The final result from `rhoCentralFoam` captures most of the features of the flow, except that the rear shock is slightly too close to the rear.

3.4 Discussions

We provide more technical and graphical details of the proposal in the Appendix.

Our validation results are quite satisfactory for the mesh level tested. Nevertheless, new algorithmic developments are desired in order to improve numerical efficiency and speedup. A robust, efficient density-based steady solver, will greatly accelerate the process as well as better shocks capturing. In fact, Shen, et al implemented a density-based LU-SGS implicit solver in OpenFOAM, which is not subject to strict CFL condition [27]. There might be other methods to be explored in this regard. Meanwhile, further testing and mesh convergence study need to be conducted.

4 Outlook

The R&D of CFD is a required leading technology for ultra modern high-performance aircraft design by Airbus, Boeing and other leading aircraft designers of the world. Further extensions and generalizations to hypersonic aircraft designs will follow up as a natural continuation of this project. The study of BWB and CFD by this KSU-CityU collaborative team promises to provide leadership to the Kingdom of Saudi Arabia's technological diversification efforts in aerospace and also for many other important engineering projects related to fluid dynamics.

References

- [1] T. Risch, G. Cosentino, C. D Regan, M. Kisska, and N. Princen, *X-48b flight-test progress overview*, 47th aiaa aerospace sciences meeting including the new horizons forum and aerospace exposition, 2009.
- [2] R. H Liebeck, *Design of the blended wing body subsonic transport*, Journal of aircraft **41** (2004), no. 1, 10–25.
- [3] S. Wakayama, *Blended-wing-body optimization problem setup*, AIAA Paper **4740** (2000), 2000.
- [4] D. Roman, R. Gilmore, and S. Wakayama, *Aerodynamics of high-subsonic blended-wing-body configurations*, AIAA Paper **554** (2003), 2003.
- [5] A. Morris, P Arendsen, G LaRocca, M Laban, R Voss, and H Hönlinger, *Mob-a european project on multidisciplinary design optimisation*, 24th icas congress, 2004.
- [6] N. Qin, A. Vavalle, A. Le Moigne, M Laban, K Hackett, and P Weinerfelt, *Aerodynamic considerations of blended wing body aircraft*, Progress in Aerospace Sciences **40** (2004), no. 6, 321–343.
- [7] N. Qin, A. Vavalle, and A. L. Moigne, *Spanwise lift distribution for blended wing body aircraft.*, Journal of aircraft **42** (2005), no. 2, 356–365.
- [8] J. Hileman, Z. Spakovszky, M. Drela, and M. Sargeant, *Airframe design for silent aircraft*, Aiaa aerospace sciences meeting and exhibit, 2007.
- [9] J. L Felder, H. D. Kim, and G. V Brown, *Turboelectric distributed propulsion engine cycle analysis for hybrid-wing-body aircraft*, 47th aiaa aerospace sciences meeting, orlando, fl, january, 2009, pp. 5–8.
- [10] H. Kim and M.-S. Liou, *Flow simulation of n2b hybrid wing body configuration*, Aerospace sciences meeting including the new horizons forum and aerospace exposition. nashville, tennessee, 2012.
- [11] M Meheut, R Grenon, G Carrier, M Defos, and M Duffau, *Aerodynamic design of transonic flying wing configurations*, Proceeding of ceas/katnet ii conference on key aerodynamic technologies, bremen, germany, 2009.
- [12] M. Meheut, A. Arntz, and G. Carrier, *Aerodynamic shape optimizations of a blended wing body configuration for several wing planforms*, AIAA **10** (2012), no. 6.2012, 3122.
- [13] A. Bolsunovsky, N. Buzoverya, B. Gurevich, V. Denisov, A. Dunaevsky, L. Shkadov, O. Sonin, A. Udzhuhu, and J. Zhurihin, *Flying wing problems and decisions*, Aircraft design **4** (2001), no. 4, 193–219.
- [14] J. van Dommelen and R. Vos, *Conceptual design and analysis of blended-wing-body aircraft*, Proceedings of the Institution of Mechanical Engineers, Part G: Journal of Aerospace Engineering **228** (2014), no. 13, 2452–2474.
- [15] S. Peigin and B. Epstein, *Computational fluid dynamics driven optimization of blended wing body aircraft*, AIAA journal **44** (2006), no. 11, 2736–2745.
- [16] N. B Kuntawala, *Aerodynamic shape optimization of a blended-wing-body aircraft configuration*, Ph.D. Thesis, 2011.
- [17] L. Peifeng, B. Zhang, C. Yingchun, Y. Changsheng, and L. Yu, *Aerodynamic design methodology for blended wing body transport*, Chinese Journal of Aeronautics **25** (2012), no. 4, 508–516.
- [18] Z. Lyu and J. R. Martins, *Aerodynamic design optimization studies of a blended-wing-body aircraft*, Journal of Aircraft **51** (2014), no. 5, 1604–1617.
- [19] E. Ordoukhanian and A. M Madni, *Blended wing body architecting and design: Current status and future prospects*, Procedia Computer Science **28** (2014), 619–625.
- [20] H. Jasak, A. Jemcov, and Z. Tukovic, *Openfoam: A c++ library for complex physics simulations*, International workshop on coupled methods in numerical dynamics, 2007, pp. 1–20.
- [21] G. Chen, Q. Xiong, P. J Morris, E. G Paterson, A. Sergeev, and Y Wang, *Openfoam for computational fluid dynamics*, Notices of the American Mathematical Society **61** (2014), no. 4, 354–363.
- [22] A. Kurganov and E. Tadmor, *New high-resolution central schemes for nonlinear conservation laws and convection–diffusion equations*, Journal of Computational Physics **160** (2000), no. 1, 241–282.
- [23] J. L Steger and D. S Chaussee, *Generation of body-fitted coordinates using hyperbolic partial differential equations*, SIAM Journal on Scientific and Statistical Computing **1** (1980), no. 4, 431–437.
- [24] V Schmitt and F Charpin, *Pressure distributions on the onera-m6-wing at transonic mach numbers*, Experimental data base for computer program assessment **4** (1979).
- [25] T.-W. Kim, S.-J. Oh, and K.-J. Yee, *Verification of the open source code, openfoam to the external flows*, Journal of the Korean Society for Aeronautical & Space Sciences **39** (2011), no. 8, 702–710.
- [26] U. A. Rahman and F. Mustapha, *Validations of openfoam steady state compressible solver rhosimplefoam*, International conference on mechanical and industrial engineering, 2015.
- [27] C. Shen, X.-l. Xia, Y.-z. Wang, F. Yu, and Z.-w. Jiao, *Implementation of density-based implicit lu-sgs solver in the framework of openfoam*, Advances in Engineering Software **91** (2016), 80–88.

Appendix: Meshes, Validation and Graphics

Here, we provide descriptions of testing meshes and graphical results as illustrations of our validation work

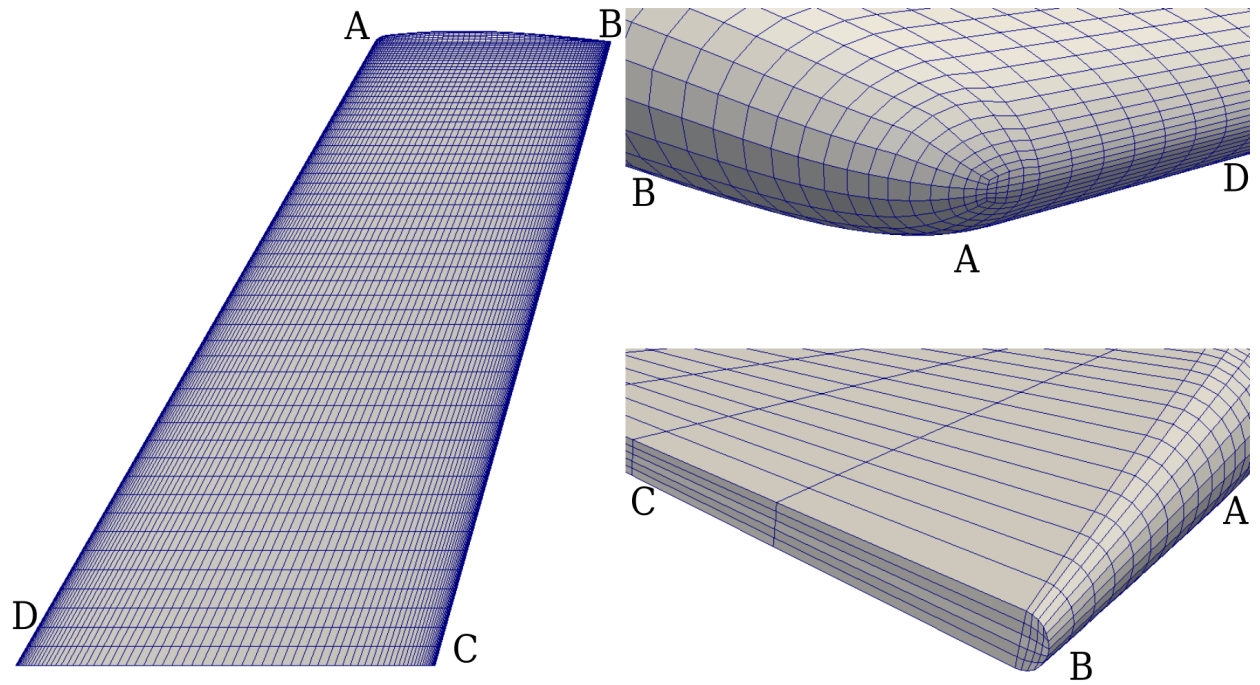


Figure 4: multi-block transfinite surface mesh for the ONERA M6 wing. The number of cells on the surface is 10,717.

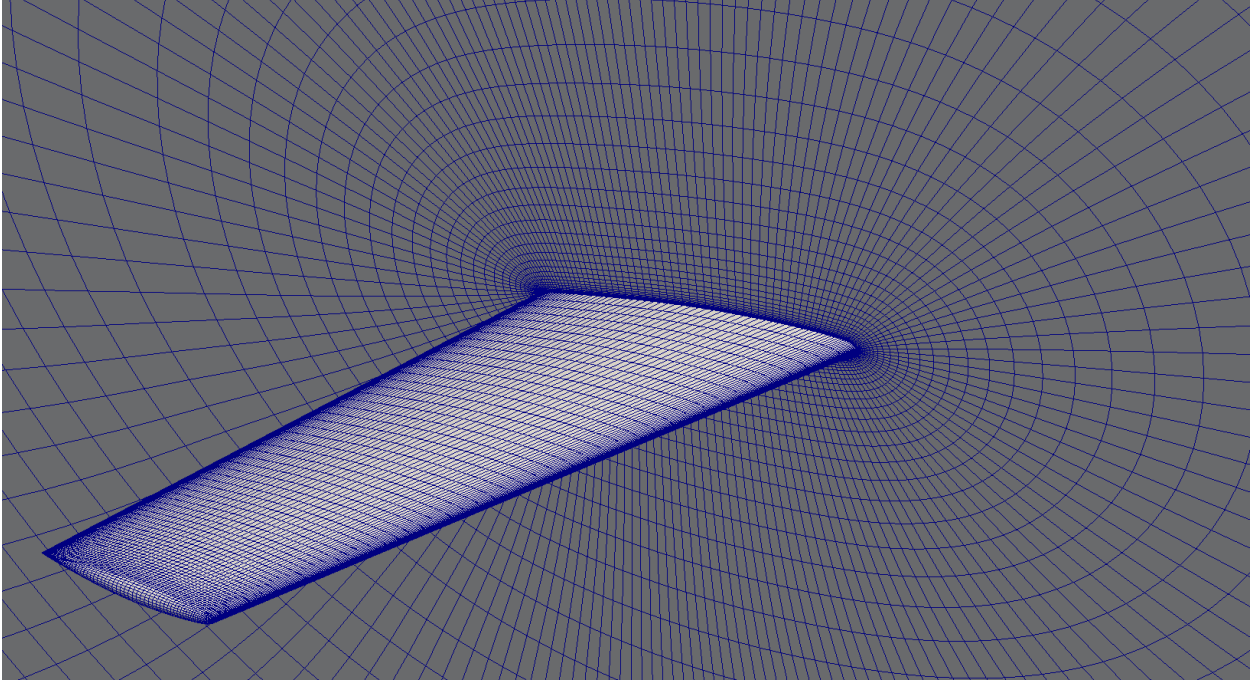


Figure 5: O-topology mesh extruded from the wing surface of ONERA M6. The number of layers in the extrusion direction is 60, with an expansion rate of 1.3. Total number of cells is 643k. The average volume of the first layer cells is 2 mm^3 , which is corresponding to a y^+ value close to 3.

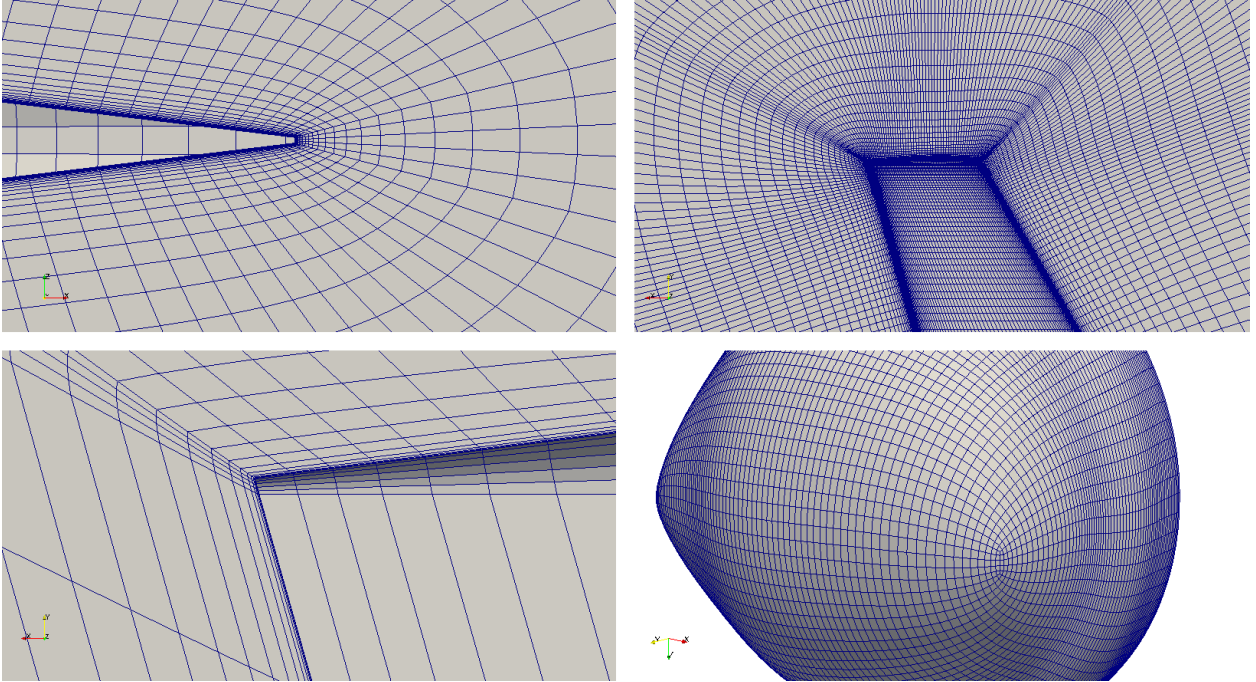


Figure 6: Details of the O-topology mesh. The lower-right subfigure shows the final (outermost) layer of the mesh.

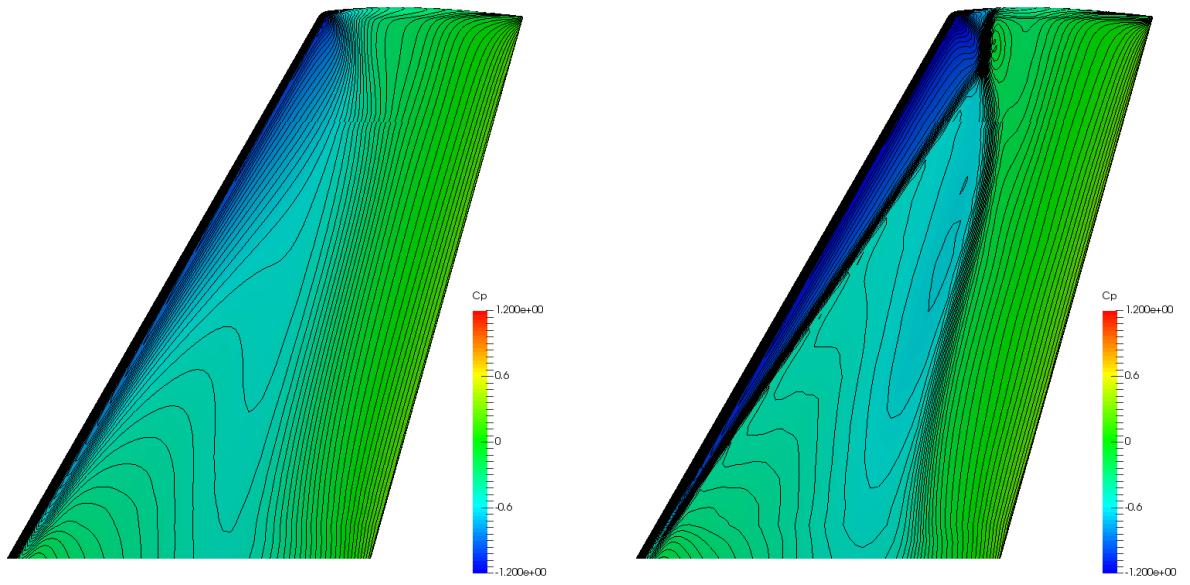


Figure 7: Pressure Coefficient (C_p) contour for the upper surface of ONERA M6. The left figure shows the converged result of `rhoSimpleFoam` with upwind scheme. The right figure shows the result of `rhoCentralFoam` with the Kurganov scheme.

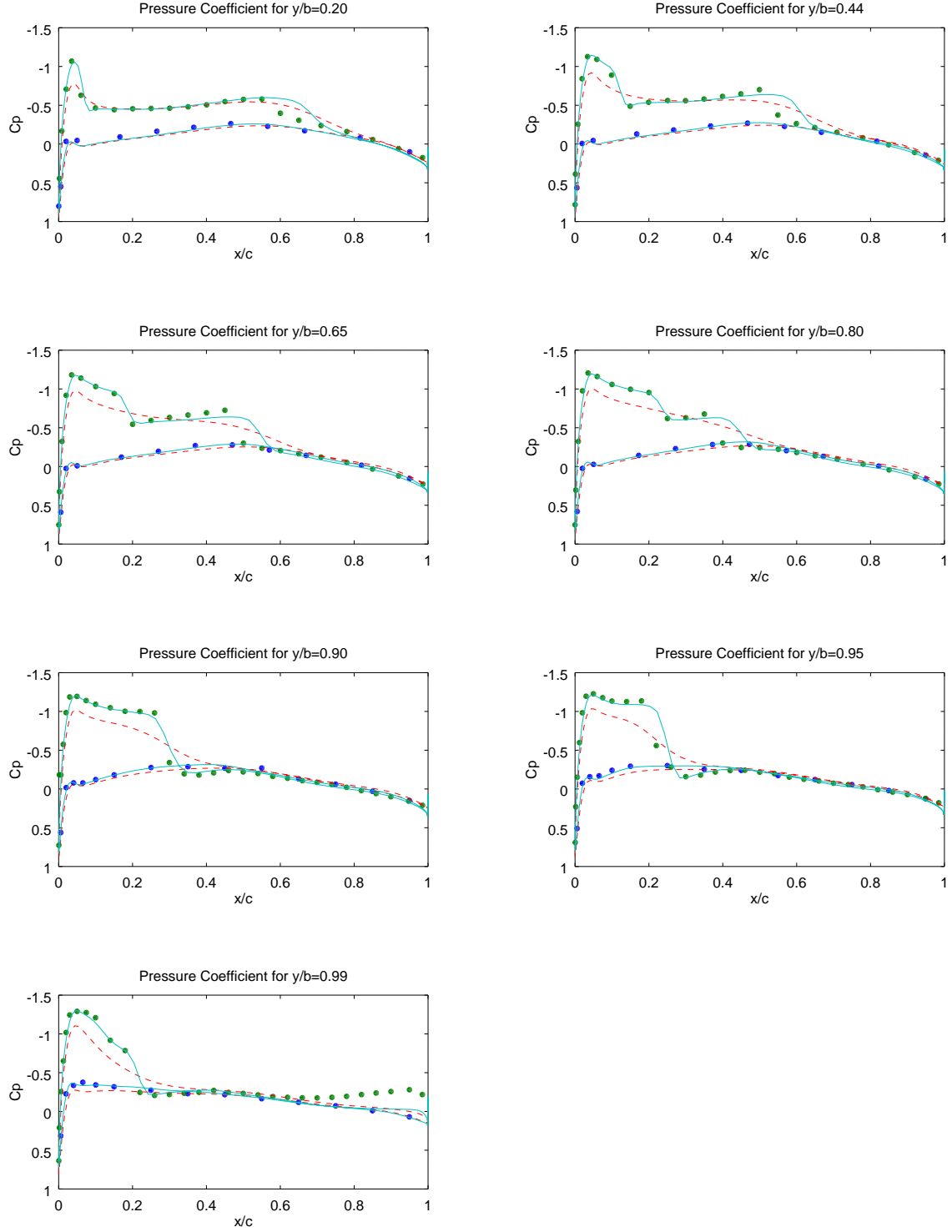


Figure 8: Pressure Coefficient (C_p) along different span locations in comparison with experimental data for ONERA M6. The dots are data points from the experiment. The dashed line is the converged result of `rhoSimpleFoam` with an upwind scheme. The solid line is the result of `rhoCentralFoam` with the Kurganov scheme.